Available online at www.sciencedirect.com
ScienceDirect
Journal of Solid State Chemistry 179 (2006) 3437–3444
JOURNAL OF SOLID STATE CHEMISTRY
www.elsevier.com/locate/jssc

Phase relations and crystal structures in the systems $(Bi,Ln)_2WO_6$ and $(Bi,Ln)_2MoO_6$ (Ln = lanthanide)

Peter S. Berdonosov[a], Dmitri O. Charkin[b], Kevin S. Knight[c], Karen E. Johnston[d], Richard J. Goff[d], Valeriy A. Dolgikh[a], Philip Lightfoot[d,*]

[a]*Department of Chemistry, Moscow State University, 119992 Moscow GSP-2, Russia*
[b]*Department of Materials Sciences, Moscow State University, 119992 Moscow GSP-2, Russia*
[c]*ISIS Facility, Rutherford Appleton Laboratory, Chilton, Oxon OX11 0QX, UK*
[d]*School of Chemistry, University of St. Andrews, St. Andrews KY16 9ST, UK*

Received 19 June 2006; accepted 7 July 2006
Available online 12 July 2006

Abstract

Several outstanding aspects of phase behaviour in the systems $(Bi,Ln)_2WO_6$ and $(Bi,Ln)_2MoO_6$ (Ln = lanthanide) have been clarified. Detailed crystal structures, from Rietveld refinement of powder neutron diffraction data, are provided for $Bi_{1.8}La_{0.2}WO_6$ (L-Bi_2WO_6 type) and $BiLaWO_6$, $BiNdWO_6$, $Bi_{0.7}Yb_{1.3}WO_6$ and $Bi_{0.7}Yb_{1.3}WO_6$ (all H-Bi_2WO_6 type). Phase evolution within the solid solution $Bi_{2-x}La_xMoO_6$ has been re-examined, and a crossover from γ(H)-Bi_2MoO_6 type to γ-R_2MoO_6 type is observed at $x\sim1.2$. A preliminary X-ray Rietveld refinement of the line phase $BiNdMoO_6$ has confirmed the α-R_2MoO_6 type structure, with a possible partial ordering of Bi/Nd over the three crystallographically distinct R sites.

Keywords: Bismuth oxides; Molybdates; Tungstates; Ferroelectric; Neutron diffraction

1. Introduction

Phase equilibria in complex oxides of the formula $Bi_{2-x}Ln_xMO_6$ (M = Mo^{6+} or W^{6+}) have been studied by a number of previous authors, and several key phases have been isolated and characterized. Despite this, however, several of the known phases remain poorly characterized structurally and certain aspects of solid solution formation remain unresolved.

The parent phases of the above series, Bi_2WO_6 and Bi_2MoO_6 are known to have three polymorphic phases as a function of temperature. At room-temperature both are ferroelectric, and adopt the orthorhombic Aurivillius structure, consisting of alternating fluorite-like $[Bi_2O_2]^{2+}$ layers and $[MO_4]^{2-}$ layers comprising corner-linked octahedral units (Fig. 1(a)). In the case of Bi_2WO_6, the intermediate-temperature (I) form has a higher (orthorhombic) symmetry, but essentially the same connectivity, whereas the high-temperature (H) monoclinic form (Fig. 1(b)) retains the layered nature but the $[MO_4]^{2-}$ layers now comprise edge-linked chains of octahedra [1]. In the case of Bi_2MoO_6, the three polymorphs are generally referred to as γ, γ'' and γ', or γ(L), γ(I) and γ(H) for the low-, intermediate- and high-temperature forms, respectively [2–4]. As with Bi_2WO_6 the (L) and (I) forms have closely related orthorhombic structures based on the Aurivillius phases, but the γ(H) form has a very complex monoclinic ($P2_1/c$) structure (Fig. 1(c)) which has been described as 'columnar' rather than layered structure and contains isolated tetrahedral MoO_4^{2-} units [5,6]. In addition to these three forms an additional fluorite-related phase has been proposed, prepared by mechanochemical activation [7].

At the opposite end of the $(Bi_{2-x}Ln_x)MO_6$ solid solution series there are several known structure types, depending on the nature of Ln and M. La_2MoO_6 has a tetragonal structure closely related to the Aurivillius phases, with analogous fluorite-like $[La_2O_2]^{2+}$ layers, but in this case the $[MO_4]^{2-}$ layers consist of isolated MoO_4^{2-} tetrahedra (Fig. 1(d)) [8]. The high-temperature forms of Pr_2MoO_6

*Corresponding author. Fax: +44 1334 463808.
E-mail address: pl@st-and.ac.uk (P. Lightfoot).

0022-4596/$ - see front matter © 2006 Elsevier Inc. All rights reserved.
doi:10.1016/j.jssc.2006.07.008

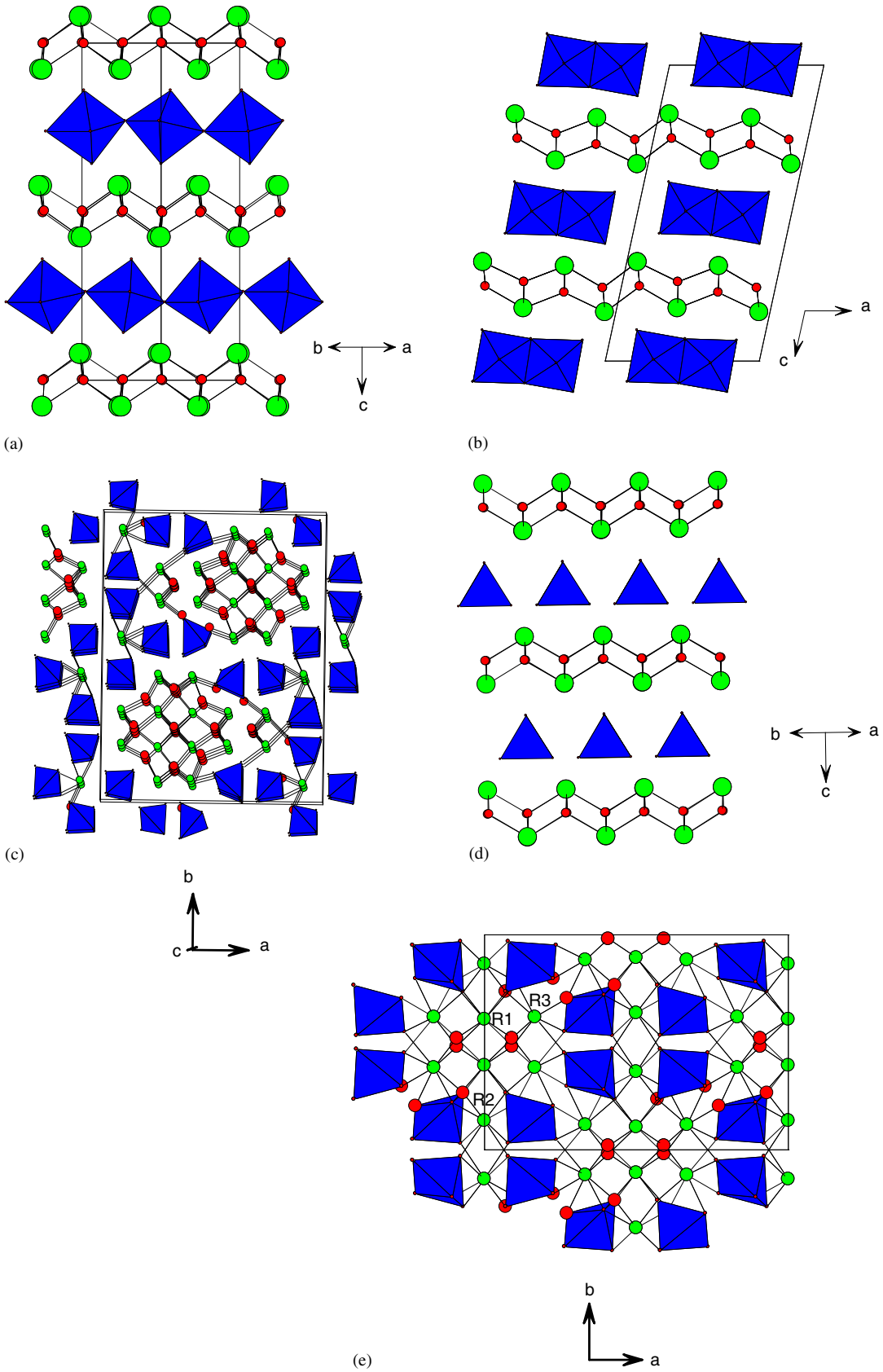

Fig. 1. (a) The structure of L-Bi_2WO_6, space group $P2_1ab$; (b) the structure of H-Bi_2WO_6, space group $A2/m$; (c) the structure of γ(H)-Bi_2MoO_6, space group $P2_1/c$; (d) the structure of La_2MoO_6, space group $I4_1/acd$. Note only a portion of the unit cell along the c-axis is shown; and (e) the structure of α-R_2MoO_6, space group $C2/c$.

and Nd_2MoO_6 also adopt this structure type (γ-R_2MoO_6), whereas Ce_2MoO_6 adopts a pseudo-cubic fluorite-like structure (β polymorph), the details of which are still unknown. The smaller trivalent lanthanide derivatives adopt the so-called α-R_2MoO_6 structure which has a complex fluorite-related superstructure (monoclinic, $C2/c$) featuring isolated MoO_5 polyhedra (Fig. 1(e)) [9,10]. The crystal chemistry of the lanthanide tungstates, Ln_2WO_6, is more extensive. According to Tyulin and Efremov [11], there are seven polymorhpic forms: tetragonal I, whose structure is unknown, is observed for La; monoclinic II (Ce–Ho, Y) is identical to α-R_2MoO_6. The other forms (III–VII) seem to be structurally quite different from the corresponding Ln_2MoO_6. In many cases, mixtures of different polymorphs are obtained in solid-state synthesis, and pure forms can be obtained by careful selection of sintering temperature, time, cooling rate, and even the rate of solvent (molten alkali halide) evaporation.

Various studies have been performed on solid solutions of the type $Bi_{2-x}Ln_xMO_6$. For M = W, Watanabe reported an intermediate phase over a range of compositions for all lanthanides (approximate limits $0.3<x<1.3$) [12]. We have recently confirmed this phase to be isotypic to the H-Bi_2WO_6 structure and have carried out a detailed analysis of the structure of $Bi_{0.7}Yb_{1.3}WO_6$ by powder neutron diffraction [13]. For M = Mo, the H-Bi_2WO_6 structure type also exists for $Bi_{2-x}Ln_xMO_6$ for M = Gd–Lu and Y, and $1.15<x<1.4$ [14]. The α-R_2MoO_6 structure has been reported for the above series at $0.4<x<0.7$ and also for $BiNdMoO_6$ [15]. For Ln = La, an early study suggested an extensive solid solution of γ-Bi_2MoO_6 type for low x values, and very small solid solution range of γ-R_2MoO_6 type at high x [16]. This work was to some extent contradicted by Bode et al. [17], who suggested a solid solution of γ-R_2MoO_6 type over the range $1.2<x<2$. The work of Khaikina et al. [15] suggested a similar stability range for the γ-R_2MoO_6 phase in $Bi_{2-x}Nd_xMO_6$, together with a solid solution of γ(H)-Bi_2MoO_6 type rather than γ(L)-Bi_2MoO_6 type at low x values.

The purpose of this paper is to clarify some of the issues remaining open in these systems, in particular to present more accurate and reliable structural data for some solid solution phases of the L-Bi_2WO_6 and H-Bi_2WO_6 type, and to clarify the nature of the phases present in the $Bi_{2-x}La_xMoO_6$ and $Bi_{2-x}Nd_xMoO_6$ systems.

2. Experimental

Polycrystalline samples were prepared by conventional solid-state reaction in alumina crucibles in air. High purity (>99.9%) starting reagents, Bi_2O_3, WO_3, MoO_3 and Ln_2O_3, were dried thoroughly prior to use. Typically, for the tungstates, the heating regime was 1000 °C for 3–4 days with one intermediate regrinding. Bi_2MoO_6 was initially prepared at 580 °C due to the anticipated sample volatility; this resulted in preparation of the pure γ(L)-polymorph. However, even upon doping of small amounts of lanthanide, this temperature proved insufficient to ensure satisfactory reaction. Targeting Bi_2MoO_6, a reaction temperature of 900 °C produced phase-pure γ(H)-polymorph. For the lanthanide-containing molybdates, a temperature of 900 °C was used, with samples being reacted for up to 5 days, with intermediate regrinding, as required to ensure complete reaction. On completion of the reaction, samples were removed from the furnace and allowed to cool rapidly in air. Later, several slow-cooling regimes were attempted (unsuccessfully) in order to explore the scope for stabilizing the low-temperature polymorphs of $Bi_{2-x}La_xMoO_6$.

Powder X-ray diffraction data were collected on a Stöe STADI/P diffractometer operating in transmission geometry, with Cu$K\alpha_1$ radiation. Data suitable for Rietveld refinement were collected for about 15 h over a 2θ range 5–100°. Powder neutron diffraction data were collected at the ISIS Facility, using the high-resolution or high-flux instruments HRPD and Polaris. Approximately 10 g powder samples were loaded into cylindrical vanadium cans. Details of data collections and analyses are given in Table 1.

3. Results

3.1. Neutron structure of $Bi_{1.8}La_{0.2}WO_6$ (L-Bi_2WO_6 type)

In the system $Bi_{2-x}La_xWO_6$, Watanabe et al. [18] reported a solid solution of L-Bi_2WO_6 type up to around $x\sim0.2$, followed by a solid solution of H-Bi_2WO_6 type for $0.4<x<1.0$. In order to confirm the structural details of the first solid solution we carried out a powder neutron diffraction Rietveld study of $Bi_{1.8}La_{0.2}WO_6$. Previous neutron diffraction studies [1,19] had confirmed a subtle lowering of symmetry in ferroelectric Bi_2WO_6 from the archetypal space group $B2cb$ to $P2_1ab$. In this study, we tested both models carefully. Our results clearly show that the lower symmetry $P2_1ab$ structure is retained for $Bi_{1.8}La_{0.2}WO_6$, which results in a markedly better fit ($P2_1ab$: $\chi^2 = 12.4$, $R_{wp} = 0.028$ for 45 variables; $B2cb$: $\chi^2 = 38.6$, $R_{wp} = 0.048$ for 28 variables). In particular, reflections violating B-centering can be clearly seen. Details of this refinement are provided in Table 1 and Fig. 2. Full details of the refinement are provided in the deposited data. There are no major differences in geometry as compared to Bi_2WO_6 itself.

3.2. Neutron structures of some phases of the H-Bi_2WO_6 type

We first reported a detailed analysis of this structure type in the form of $Bi_{0.7}Yb_{1.3}WO_6$, using high-resolution powder neutron diffraction data [13], followed by the solution of the H-Bi_2WO_6 structure itself [1]. The essential features of these structures are the same, viz. $[Bi_2O_2]^{2+}$ layers of the Aurivillius-type alternating with $[MO_4]^{2-}$

Table 1
Powder neutron diffraction data collection and refinement details

Sample	$Bi_{1.8}La_{0.2}WO_6$	$Bi_{0.7}Yb_{1.3}WO_6$	$BiLaWO_6$	$BiNdWO_6$	$Bi_{0.7}Yb_{1.3}MoO_6$
Instrument	Polaris	Polaris	Polaris	HRPD	HRPD
Data range (Å)	0.4–3.08	0.45–3.08	0.45–3.08	0.66–4.1	0.85–2.52
No. of parameters	45	56	54	49	47
R_{wp}, $R(F^2)$	0.028, 0.080	0.031, 0.052	0.040, 0.080	0.073, 0.167	0.115, 0.94
Space group	$P2_1ab$	$A2/m$	$A2/m$	$A2/m$	$A2/m$
a (Å)	5.4410(1)	8.1064(2)	8.3213(3)	8.24542(7)	8.02422(6)
b (Å)	5.4282(1)	3.7050(1)	3.8647(2)	3.81854(4)	3.75424(4)
c (Å)	16.4366(2)	15.8430(7)	16.5103(8)	16.3085(2)	15.7356(3)
β (°)	90	103.536(3)	102.239(4)	102.270(1)	103.153(1)

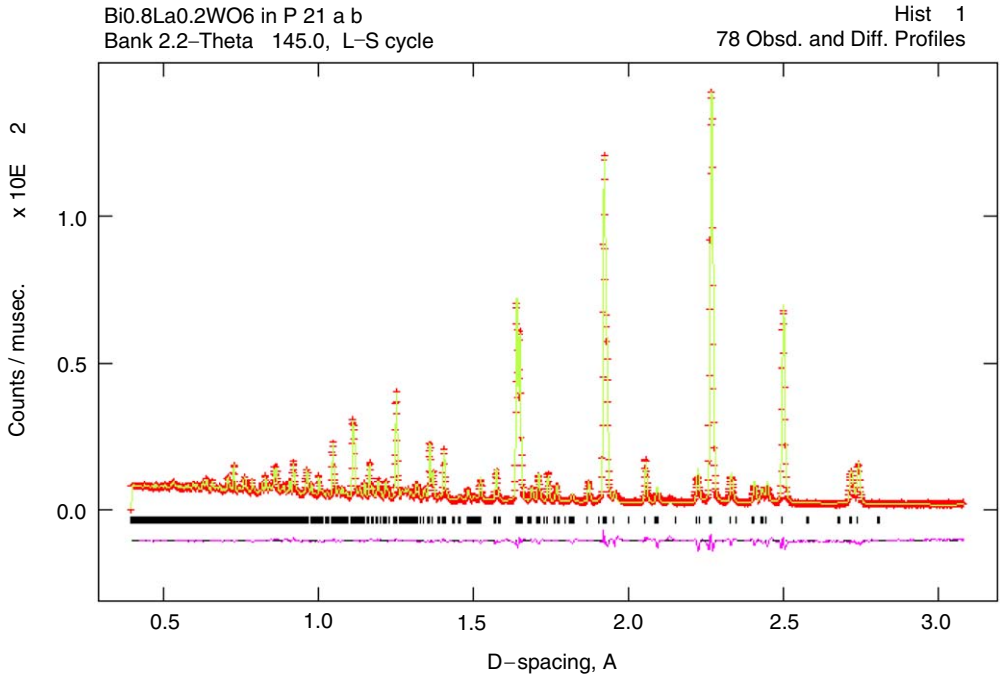

Fig. 2. Final Rietveld fit (Polaris) for $Bi_{1.8}La_{0.2}WO_6$ (L-Bi_2WO_6 type), space group $P2_1ab$.

layers comprising edge-linked chains of octahedra. H-Bi_2WO_6 refines very well in space group $A2/m$, with no disorder. However, in our earlier study we suggested a possible lowering of symmetry in $Bi_{0.7}Yb_{1.3}WO_6$ to non-centrosymmetric space group $A2$, with some concomitant disorder. We have now analysed several related compositions of this structure type, and here suggest a significantly improved model, which retains the centrosymmetric $A2/m$ space group, but involves additional disorder around the octahedral MO_6 site (Table 2). The results of powder neutron diffraction Rietveld refinements, using the same structural model for each of these phases are presented in Tables 1 and 2 and Fig. 3. Full details of each refinement are provided in the deposited data. The idealized structure is shown in Fig. 1(b). The disorder model involves two-fold rotational disorder of the MO_6 octahedron around the a-axis (Fig. 4). Due to this inherent disorder, it is difficult to draw any meaningful trends in structural behaviour across the series. This study confirms the existence of the H-Bi_2WO_6 structure type over an extended range of compositions in the (Bi,Ln)$_2WO_6$ family and also in a representative of the corresponding (Bi,Ln)$_2$-

Table 2
Final atomic parameters for $BiNdWO_6$ (H-Bi_2WO_6 type)

Atom	x	y	z	$U_{iso} \times 100$
Bi/Nd(1)[a]	0.9230(3)	0.0	0.3319(2)	1.21(4)
Bi/Nd(2)[a]	0.3965(3)	0.00	0.32077(17)	1.21(4)
W(1)[b]	0.2967(5)	0.445(2)	0.4974(3)	1.6(2)
O(1)	0.1188(4)	0.0	0.2489(3)	1.8(1)
O(2)	0.3640(4)	0.5	0.2338(2)	1.3(1)
O(3)[b]	0.3224(9)	0.0	0.5284(5)	1.0(1)
O(4)[b]	0.5068(4)	0.438(2)	0.5745(3)	0.7(1)
O(5)[b]	0.1709(5)	0.414(1)	0.5669(3)	1.1(1)
O(6)[b]	0.1664(5)	0.609(1)	0.3992(3)	0.6(1)
O(3a)[b]	0.2978(8)	0.0	0.4628(4)	1.0(1)

[a]Occupancies fixed at 50:50.
[b]50% occupancy.

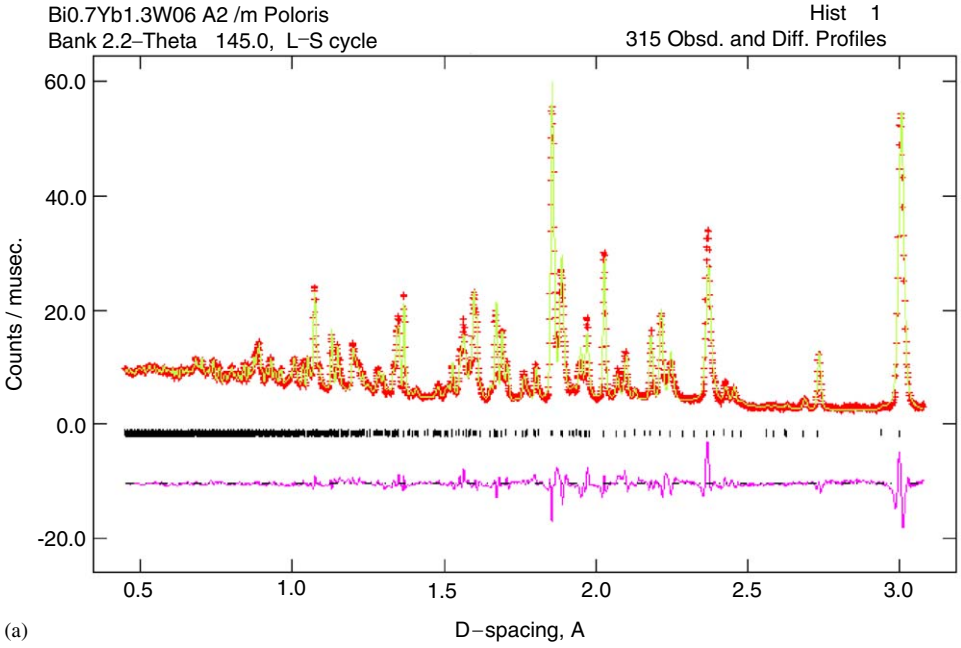

Fig. 3. (a) Final Rietveld fit (Polaris) for $Bi_{0.7}Yb_{1.3}WO_6$ (H-Bi_2WO_6 type), space group $A2/m$; (b) final Rietveld fit (HRPD) for $BiNdWO_6$ (H-Bi_2WO_6 type), space group $A2/m$.

MoO_6 series. It is unclear why the lanthanide-doped derivatives exhibit disorder around the octahedral site, whereas Bi_2WO_6 does not. In the case of the (Bi,Yb) examples the neutron scattering contrast is sufficient to determine significant site-preference differences between the two cations (this is not feasible for the (Bi,La) and (Bi,Nd) samples: neutron scattering lengths (fm): Bi: 8.532, Yb: 12.43, La: 8.24, Nd: 7.69). However, there is no evidence of further superlattice ordering, suggesting that the octahedral disorder is simply due to localized bonding competition at the Bi/*Ln* sites.

3.3. *Phase evolution in $Bi_{2-x}La_xMoO_6$*

The original study of Vyawahare and Chincholkar [16] suggested that Bi-doping into La_2MoO_6 produced γ(L)-Bi_2MoO_6 as a secondary phase, along with tetragonal La_2MoO_6, even at Bi concentration as low as 10%. They

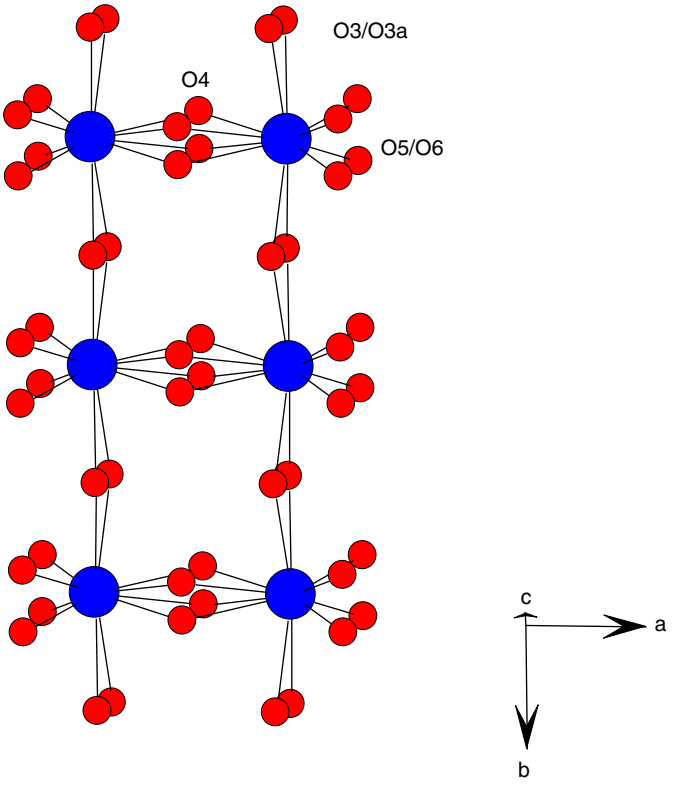

Fig. 4. Disorder of the octahedral MO_6 chains in $BiNdWO_6$ (and related structures)—H-Bi_2WO_6 structure type.

suggested that the two-phase mixture persisted across the region $0.8<x<1.8$, with a γ(L)-Bi_2MoO_6-type solid solution being present as a single phase for $x = 0.8$ or less. On the contrary, Bode et al. [17] suggested a single phase solid solution of tetragonal La_2MoO_6 (γ-R_2MoO_6) type across the range $1.2<x<2.0$. In order to clarify the nature of the phases present in this system we prepared samples at x intervals of 0.2 across the complete composition range. Rietveld refinements were carried out at each compositions, using 'ideal' structural models for the parent phases but varying lattice and other profile parameters. Under the synthesis conditions employed our results reveal a single phase solid solution of tetragonal La_2MoO_6 type in the range $1.2<x<2.0$, a single phase γ(H)-Bi_2MoO_6 solid solution in the range $0<x<1.2$ and a mixture of these two phases at $x = 1.2$. This is in reasonable agreement with the results of Bode et al. but in direct conflict with those of Vyawahare. In fact, the raw X-ray powder diffraction data for γ(L)-Bi_2MoO_6 and γ(H)-Bi_2MoO_6 look surprisingly similar at first glance (shown in Fig. 5, along with the pattern for tetragonal La_2MoO_6), perhaps since they both contain 'fluorite-like' structural elements; the key features which can be used to distinguish them prior to a full Rietveld refinement are the peaks below about 25°. In an effort to produce a solid solution of the γ(L)-Bi_2MoO_6 type we tested various slow-cooling regimes, but none produced significantly different products. A complete list of refined

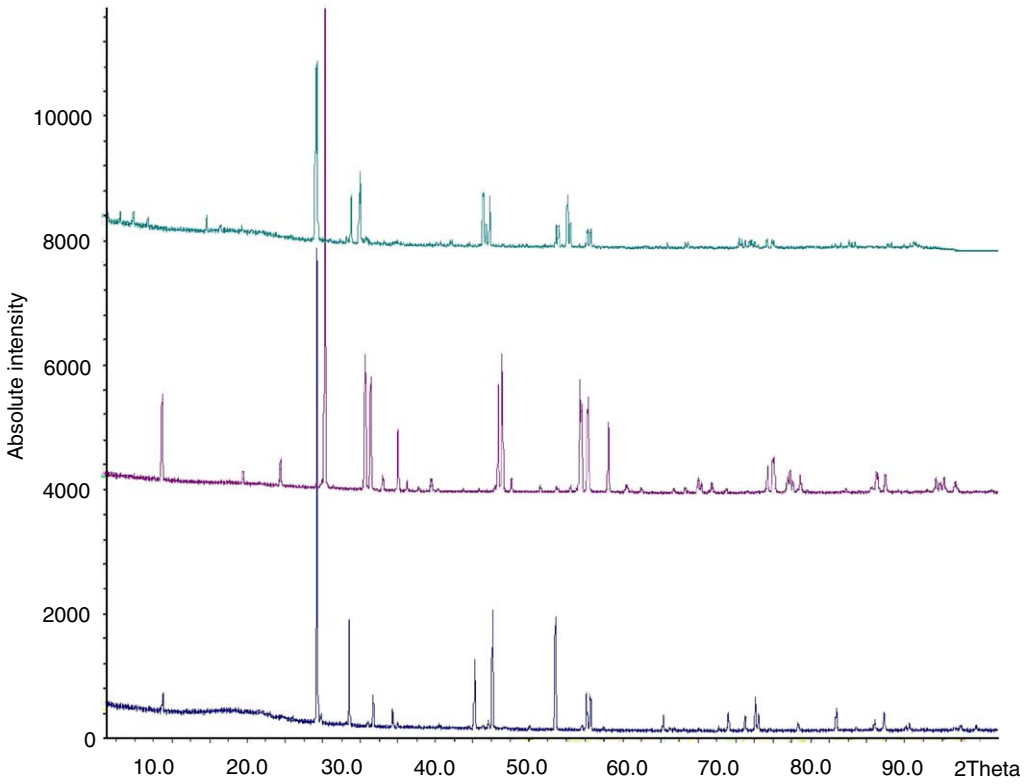

Fig. 5. Raw powder X-ray diffraction data for γ(H)-Bi_2MoO_6 (top), γ(L)-Bi_2MoO_6 (middle) and La_2MoO_6 (bottom).

lattice parameters for the full composition range is given in Table 3. The evolution of unit cell volume versus composition is shown in Fig. 6, and a typical Rietveld fit is shown in Fig. 7.

3.4. X-ray structure of $BiNdMoO_6$ (α-R_2MoO_6 type)

Khaikina et al. [15] suggested the α-R_2MoO_6 structure for $BiNdMoO_6$. This structure type has three crystallographically distinct R (i.e. Bi/Nd) sites (Fig. 1(e)) all of which have eight-fold coordination to oxygen, but of somewhat differing degrees of distortion. It is therefore of interest to ascertain whether there is any tendency towards site-ordering of Bi/Nd amongst these sites. X-ray Rietveld refinement was carried out on a sample prepared at 900 °C, using as a starting model the structure of Yb_2MoO_6 [10]. A trace amount ($\ll 5\%$) of a γ(H)-Bi_2MoO_6 polymorph was also present. Keeping the positional parameters for oxygen atoms fixed, but refining the usual unit cell and profile parameters, together with the coordinates, grouped thermal parameters and freely refined occupancies for the three R sites revealed a clear preference of Nd for the $R(1)$ site (around 90% Nd occupancy), and approximately equal preference of Nd for the remaining two sites. Although it is clearly dangerous to over-interpret this result we may tentatively suggest that Nd prefers the $R(1)$ site on the grounds of smaller ionic size, due to the presence of two significantly longer bonds (2.77 Å in Yb_2MoO_6) and six shorter bonds (2.22–2.37 Å) rather than eight intermediate bonds lengths. Alonso et al. [10] discussed the stability limits of this structure type in terms of ionic size and bond valence sum arguments and concluded that the structure was unstable for lanthanide cations larger than Dy^{3+}, due to global bonding requirements. Interestingly, the unit cell parameters of $BiNdMoO_6$ ($a = 17.2383(5)$ Å, $b = 11.5617(4)$ Å, $c = 5.6014(2)$ Å, $\beta = 110.001(1)^\circ$, $V = 1049.06(6)$ Å^3) are far in excess of those for Dy_2MoO_6 ($a = 16.4160(5)$ Å, $b = 11.0745(4)$ Å, $c = 5.3734(2)$ Å, $\beta = 108.385(2)^\circ$, $V = 927.01(5)$ Å^3). A more detailed analysis of this structure by single crystal X-ray or powder neutron diffraction would be required in order to rationalize the extension of this stability window by the incorporation of bismuth.

Table 3
Rietveld refined lattice parameters for phases in the $Bi_{2-x}La_xMoO_6$ system

x	a (Å)	b (Å)	c (Å)	β (deg)	V (Å^3)
0.0[a]	5.50481(6)	5.40378(6)	16.2108(2)		489.36(1)
	17.2587(4)	22.4238(6)	5.5845(1)	90.495(2)	2161.2(1)
0.2	17.2781(4)	22.5118(5)	5.6010(1)	90.492(1)	2178.5(1)
0.4	17.2766(3)	22.5692(4)	5.5960(1)	90.340(1)	2182.0(1)
0.6	17.2944(3)	22.6245(3)	5.5972(1)	90.212(1)	2190.0(1)
0.8	17.3128(4)	22.6522(5)	5.5935(1)	90.115(2)	2193.6(1)
1.0	17.3864(4)	22.6773(6)	5.5946(2)	90.077(4)	2205.8(1)
1.2[b]	17.402(1)	22.678(2)	5.598(5)	90.104(5)	2209.2(2)
	5.73760(6)		32.2477(4)		1061.60(3)
1.4	5.74742(8)		32.2385(6)		1064.93(4)
1.6	5.76725(8)		32.1946(6)		1070.83(4)
1.8	5.7880(1)		32.1254(8)		1076.24(5)
2.0	5.78862(9)		32.1412(7)		1076.99(5

[a]Either γ(L)-Bi_2MoO_6 and γ(H)-Bi_2MoO_6 polymorphs (note the significant difference in density: γ(H)—7.50 g cm^{-3}, γ(L)—8.28 g cm^{-3}).
[b]Mixture of γ(H)-Bi_2MoO_6 and γR_2MoO_6 polymorphs.

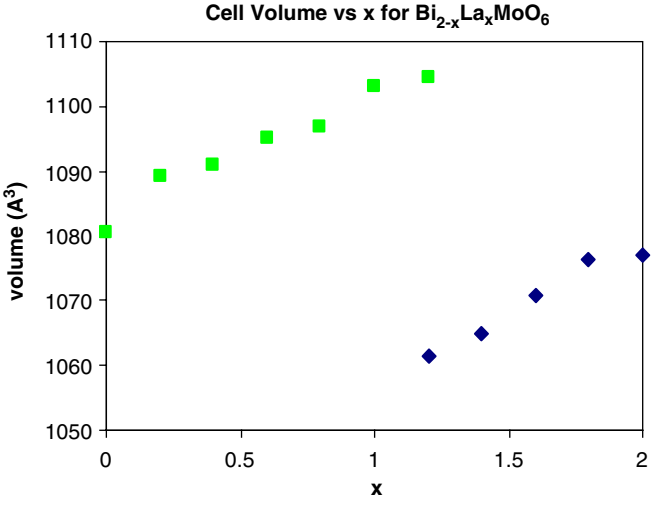

Fig. 6. Unit cell volume versus x for the system $Bi_{2-x}La_xMoO_6$. For $0 < x < 1.2$, the data refer to the γ(H)-Bi_2MoO_6 model; for $1.2 < x < 2.0$ the data refer to the La_2MoO_6 model; for $x = 1.2$ a two phase mixture was refined. The unit cell volume for the γ(H)-Bi_2MoO_6 phase is divided by 2 for ease of comparison.

4. Conclusions

The aim of this paper has been to summarize and clarify certain issues regarding phase compositions and crystal structures in the systems $(Bi,Ln)_2WO_6$ and $(Bi,Ln)_2MoO_6$. Detailed structural models of examples of two of the polymorphs in these systems have been provided from powder neutron diffraction data. In particular, the H-Bi_2WO_6 structure type, which occurs over a wide solid-solubility window in the $(Bi,Ln)_2WO_6$ system, and to a lesser extent in the corresponding Mo-based series, has been shown to accommodate Ln^{3+} for Bi^{3+} substitution via disordering of the octahedral sites, though probably retaining the same space group symmetry as the archetypal H-Bi_2WO_6. In addition, clarification of the phase evolution within the $Bi_{2-x}La_xMoO_6$ system has been given, together with a partial structural model for the α-R_2MoO_6 phase $BiNdMoO_6$. The exact nature of the structure of La_2WO_6 remains one of the outstanding issues in this area.

Further details of the structure refinements have been deposited at Fachinformationszentrum, Karlsruhe, e-mail: crysdata@fiz.karlsruhe.de.

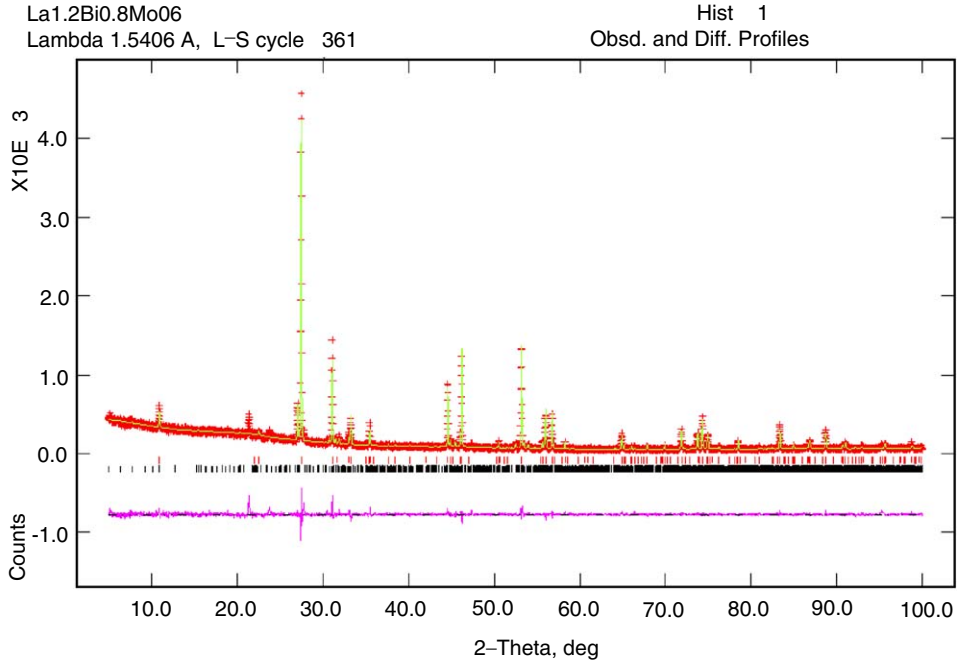

Fig. 7. Final X-ray Rietveld fit for $Bi_{0.8}La_{1.2}MoO_6$ (two phase model—89% La_2MoO_6-type, 11% γ(H)-Bi_2MoO_6-type).

Acknowledgments

We would like to thank INTAS, the Royal Society and EPSRC for financial support and Dr. R.I. Smith for assistance with neutron diffraction data collection.

References

[1] N.A. McDowell, K.S. Knight, P. Lightfoot, Chem. Eur. J. 12 (2006) 1493.
[2] H. Kodama, A. Watanabe, J. Solid State Chem. 56 (1985) 225.
[3] D.J. Buttrey, T. Vogt, B.D. White, J. Solid State Chem. 155 (2000) 206.
[4] G. Sankar, M.A. Roberts, J.M. Thomas, G.U. Kulkarni, N. Rangavittal, C.N.R. Rao, J. Solid State Chem. 119 (1995) 210.
[5] D.J. Buttrey, T. Vogt, U. Wildgruber, W.R. Robinson, J. Solid State Chem. 111 (1994) 118.
[6] P. Bégué, R. Enjalbert, J. Galy, A. Castro, Solid State Sci. 2 (2000) 637.
[7] P. Bégué, P. Millan, A. Castro, Bol. Soc. Esp. Ceram. Vidr. 38 (1999) 558.
[8] J.S. Xue, M.R. Antonio, L. Soderholm, Chem. Mater. 7 (1995) 333.
[9] T.M. Polyanskaya, S.V. Borisov, N.V. Belov, Sov. Phys. Crystallogr. 15 (1971) 636.
[10] J.A. Alonso, F. Rivillas, M.J. Martinez-Lope, V. Pomjakushin, J. Solid State Chem. 177 (2004) 2470.
[11] A.V. Tyulin, V.A. Efremov, Kristallographiya 32 (1987) 363.
[12] A. Watanabe, Mater. Res. Bull. 15 (1980) 1473.
[13] P.S. Berdonosov, D.O. Charkin, V.A. Dolgikh, S. Yu. Stefanovich, R.I. Smith, P. Lightfoot, J. Solid State Chem. 177 (2004) 2632.
[14] E.G. Khaikina, L.M. Kovba, Zh.G. Bazarova, M.V. Mokhosoev, Russ. J. Inorg. Chem. 30 (1985) 1356.
[15] E.G. Khaikina, L.M. Kovba, Zh.G. Bazarova, V.V. Khakhinov, M.V. Mokhosoev, Russ. J. Inorg. Chem. 30 (1985) 1358.
[16] A.R. Vyawahare, V.S. Chincholkar, Curr. Sci. 40 (1971) 154.
[17] J.H.G. Bode, H.R. Kuijt, M.A.J.T. Lahey, G. Blasse, J. Solid State Chem. 8 (1973) 114.
[18] A. Watanabe, Y. Sekikawa, F. Izumi, J. Solid State Chem. 41 (1982) 138.
[19] K.S. Knight, Mineral. Mag. 6 (1992) 359.